Advance Sustainable Science, Engineering and Technology (ASSET)
Vol. 8, No.2, April 2026, pp. 0260207-01 ~ 0260207-012
ISSN: 2715-4211 DOI: https://doi.org/10.26877/asset.v8i2.2652

In Vitro Degradation and Mechanical Performance of Mg AZ31B for Biodegradable Bone Implant Applications

Slamet Saefudin*, Purnomo, Muhammad Subri, M. Edi Pujianto, Ilham Yustar Afif, Samsudi Raharjo

Faculty of Engineering and Computer Science, Universitas Muhammadiyah Semarang, Jl. Kedungmundu Raya No. 18 Semarang 50273, Central Java, Indonesia

*slametsaefudin66@unimus.ac.id

Abstract. Magnesium AZ31B is a promising biodegradable implant material due to its mechanical properties comparable to natural bone and its ability to degrade in physiological environments, potentially eliminating the need for secondary surgery. However, its rapid degradation can cause a significant loss of mechanical integrity, limiting its use in load-bearing applications. This study investigates the evolution of mechanical properties and surface characteristics of AZ31B during in-vitro immersion in Simulated Body Fluid (SBF). Tensile tests were conducted on triplicate specimens after immersion for 3, 6, and 9 days, while surface morphology and corrosion products were analyzed using SEM–EDX. In addition, pH variation and mass loss were monitored to evaluate corrosion behavior. The results show a progressive decrease in tensile strength from 279.77 ± 5.30 MPa (0 days) to 167.64 ± 2.31 MPa after 9 days of immersion, representing an overall reduction of approximately 40%. This degradation was accompanied by increased surface corrosion, mass loss, and solution alkalization. These findings provide quantitative insight into the relationship between corrosion progression and mechanical degradation of AZ31B, highlighting its time-dependent performance limitations and the need for surface modification strategies in biodegradable implant applications.

Keywords: biomaterials, magnesium AZ31B, biodegradable implants, mechanical integrity, corrosion

(Received 2025-09-15, Revised 2025-11-04, Accepted 2026-01-29, Available Online by 2026-04-15)

1. Introduction

Conventional metallic materials currently used as implants for bone fracture fixation, such as medical-grade stainless steel (SS 316L)[1,2], titanium alloys [3–5] , and cobalt chromium molybdenum alloy [6,7]. However, these materials are permanent in nature and lack biodegradability. The long-term presence of these permanent implants in the human body may lead to adverse effects, including chronic inflammation and stress shielding, as metallic implants act as foreign materials within biological tissues [8]. Consequently, secondary surgical procedures are often required to remove the implant after bone healing is complete. Such repeated surgeries increase patient trauma, prolong recovery time, and raise

healthcare costs. These limitations have driven growing interest in biodegradable metallic implants as a sustainable alternative [9].

Magnesium is a metal with biodegradable properties. It has attracted significant attention due to its good biocompatibility, natural biodegradability, and mechanical properties comparable to those of human cortical bone [10,11]. The elastic modulus of magnesium alloys is closer to that of bone than conventional implant metals, which helps mitigate stress shielding effects. However, the primary challenge limiting the clinical application of magnesium-based implants is their excessively high degradation rate in physiological environments [12]. Rapid degradation leads to premature loss of mechanical integrity, hydrogen evolution, and local alkalization, which can compromise implant performance before sufficient bone healing occurs. Therefore, numerous studies have been conducted to address this issue, one of which involves the addition of alloying elements to magnesium.

Several magnesium alloys, including AZ31, AZ91, and ZK60, have been investigated for biomedical applications [13]. These alloys generally exhibit improved corrosion resistance and mechanical stability compared to pure magnesium; however, concerns remain regarding long-term biocompatibility, cost, and the potential toxicity of alloying element. In contrast, AZ31B magnesium alloy offers a balanced combination of moderate mechanical strength, good formability, and the absence of rare-earth elements, making it attractive for cost effective and sustainable biomedical applications [14,15]. Nevertheless, compared to other magnesium alloys, systematic studies correlating the time dependent degradation behavior of AZ31B with its mechanical property deterioration under physiological conditions remain limited.

In addition to alloying element modification, various surface modification techniques such as polymer and ceramic coatings applied via dip coating [16,17], spray coating [18,19], and electrospinning [20,21] have been extensively explored. While these approaches can delay corrosion, degradation processes are not fully eliminated, and mechanical performance continues to evolve during immersion. Importantly, existing literature primarily focuses on corrosion rates or surface morphology, with comparatively fewer studies providing a quantitative correlation between degradation-induced surface changes and the progressive loss of mechanical strength during in-vitro exposure. Therefore, a clear knowledge gap exists in understanding how in-vitro degradation affects the mechanical integrity of AZ31B magnesium alloy over time and how corrosion morphology relates to mechanical deterioration. Addressing this gap is essential for predicting implant lifetime and informing the design of future surface modification strategies.

This research aims to investigate the influence of degradation on magnesium AZ31B in relation to the decline in mechanical strength. The immersion process is carried out in a Simulated Body Fluid (SBF) solution in an isolated chamber with varying durations. Changes in mass are measured by weighing the samples before and after immersion. The pH of the solution is observed during the immersion process. Subsequently, the immersed samples undergo tensile testing to assess the decrease in mechanical properties over the immersion period. Additionally, surface structure changes are characterized both macroscopically and using SEM-EDX.

2. **Methods**

Magnesium AZ31B alloy sheets with a thickness of 2 mm were used in this study. The chemical composition of the AZ31B magnesium alloy consisted of Al 3.23 wt.%, Zn 0.82 wt.%, Fe 0.08 wt.%, Mn 0.22 wt.%, Ni 0.001 wt.%, and Cu 0.001 wt.%, with Mg as the balance. Tensile specimens were machined in accordance with the ASTM B557 standard for sheet-type metallic materials [22]. The specimens had a gauge length of 25 mm, a gauge width of 6 mm, and a cross-sectional area of 12 mm^2 (Figure 1). The total surface area was estimated to be approximately 29.2 cm^2, assuming full exposure of all specimen faces and a thickness of 2 mm. For each immersion condition, three specimens (n = 3) were prepared and tested to ensure reproducibility. Prior to testing, all specimens were cleaned using ethanol and distilled water.

In-vitro degradation tests were conducted by immersing AZ31B magnesium alloy specimens in

Simulated Body Fluid (SBF) prepared according to the Kokubo and Takadama protocol [23], such that the ionic composition closely resembles that of human blood plasma (Table 1). The immersion durations were set to 3, 6, and 9 days to represent the early-stage degradation behavior of implants during the critical initial bone healing period, when mechanical integrity is still required. For each immersion duration, three specimens (n = 3) were used for mass loss measurements, pH monitoring, and subsequent mechanical testing. Each specimen was immersed in a sealed polypropylene container containing 200 mL of SBF, resulting in a solution volume-to-surface area ratio of approximately 20 mL/cm², in accordance with commonly reported practices for magnesium corrosion testing.

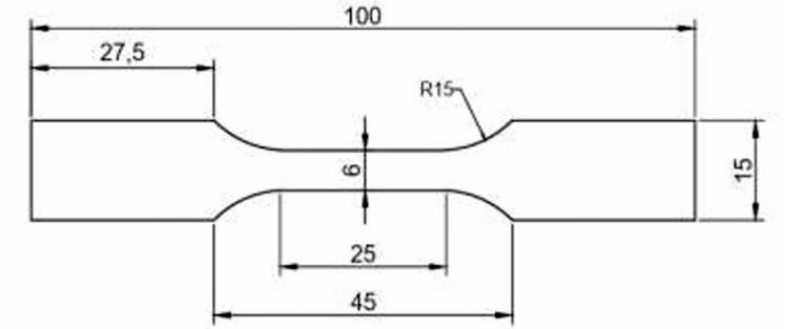

Figure 1. Specimen geometry and dimensions.

Table 1. Concentration composition of simulated body fluid

Reagent	Concentration (mMol)	Reagent	Concentration (mMol)
NaCl	136.8	$MgCL_26H_2O$	1.5
$NaHCO_3$	4.2	HCL	40
KCL	3	$CaCl_2$	2.5
$K_2HPO_43H_2O$	1	Na_2SO_4	0.5
$(CH_2OH)_3CNH_2$	50		

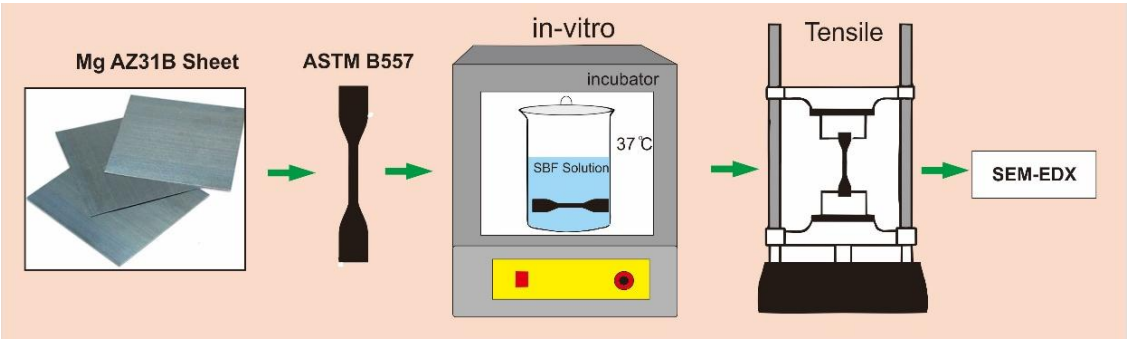

Figure 2. Research workflow

All experiments were performed under static conditions in an incubator at 37 ± 0.5 °C to simulate physiological temperature. Static SBF was employed to evaluate the intrinsic degradation behavior of AZ31B without the influence of flow-induced shear stresses. The pH of the solution was measured daily using a calibrated digital pH meter to monitor environmental changes during the degradation process. After the designated immersion periods, the specimens were carefully rinsed with distilled water and dried at room temperature for 24 h. Surface morphology and corrosion products were characterized using scanning electron microscopy coupled with energy-dispersive X-ray spectroscopy (SEM–EDX, JEOL JSM-6510LA). The corrosion rate (CR) was determined using the mass loss method following

the immersion test in simulated body fluid (SBF), in accordance with ASTM G31 [24] and ASTM G1 standards [25]. The corrosion rate (CR) was determined based on mass loss measurements and expressed in units of mg/cm²/day, where CR represents the amount of mass loss normalized by the total exposed surface area of the specimen and the immersion time. The corrosion products were then removed using a chromic acid cleaning solution in accordance with ASTM G1, prior to final weighing for accurate mass loss determination. Subsequently, the specimens were subjected to tensile testing using a universal testing machine (HT-2402) at a crosshead speed of 1 mm/min under ambient conditions (25 °C) to evaluate degradation-induced changes in mechanical properties. The overall sample preparation and testing procedure is illustrated in Figure 2.

3. Results and Discussion

Some samples that were immersed in SBF for a certain period were then taken and dried. The samples that underwent immersion experienced physical changes from their initial condition. As seen in Fig. 3, samples immersed for 3, 6, and 9 days exhibited surface changes with attached white deposits. The white deposits resulted from the reaction between the SBF solution and the metal surface. Magnesium, being the primary element in the metal, reacts with water or H_2O, producing a corrosion product in the form of $Mg(OH)_2$ [26]. Additionally, during the 6th and 9th days of immersion, the samples began to experience pitting corrosion [27]. It is observed that on the 9th day of immersion, the amount of pitting corrosion increased, leading to a decrease in mass and mechanical properties.

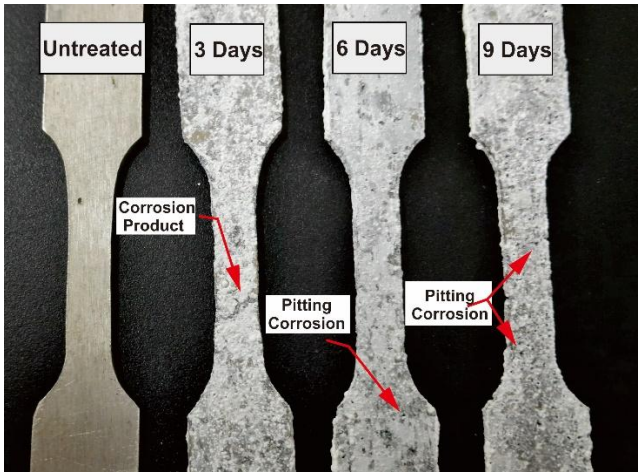

Figure 3. Changes in the sample surface after undergoing immersion

The tensile testing results on samples without immersion and with immersion in the SBF solution for different durations show changes in the tensile strength values. This is evident in Figure 4. There is a decrease in the tensile strength values with increasing immersion time. The longer the immersion time, the lower the tensile strength becomes. This is attributed to the degradation process occurring on the surface of magnesium metal with an increasing immersion time. The presence of pitting corrosion on the sample surface causes crack-prone areas to form when the sample is subjected to loading. The tensile strength value for the non-immersed sample is 274.36 N, while the lowest value occurs after 9 days of immersion, amounting to 169.32 N.

Tensile strength in the test samples experienced a decline of approximately 11%, 22%, and 38% after 3, 6, and 9 days of consecutive immersion. This reduction in strength is considerably detrimental for the application of bone implant biomaterials, as the rate of strength decrease is too rapid. Metal implants may experience functional failure before healing occurs in the injured bone area; therefore, a coating process is required to enhance mechanical strength [28], with degradable and biocompatible materials being highly recommended. In addition, the elastic modulus values increased alongside the decrease in

tensile strength values, with changes in strain values that were not significantly pronounced, as indicated in Table 2. Samples with an area of 12 mm^2 were able to withstand a maximum force of 3292.3 N under initial conditions without immersion. When converted into mass units, the use of magnesium alloy AZ31B as an implant in the leg bones can support a body weight of approximately 335.9 kg initially. However, this drastically decreases to 207.3 kg after 9 days of immersion. Based on the estimated load-bearing capacity and the observed mechanical degradation rate, AZ31B magnesium with the tested cross-sectional area is likely to experience a significant reduction in its safety margin during the early period of implantation. Although this estimation is simplified and does not yet account for the complex in-vivo loading conditions, the results highlight the importance of surface modification strategies to delay degradation and ensure adequate mechanical support throughout the bone healing process [29].

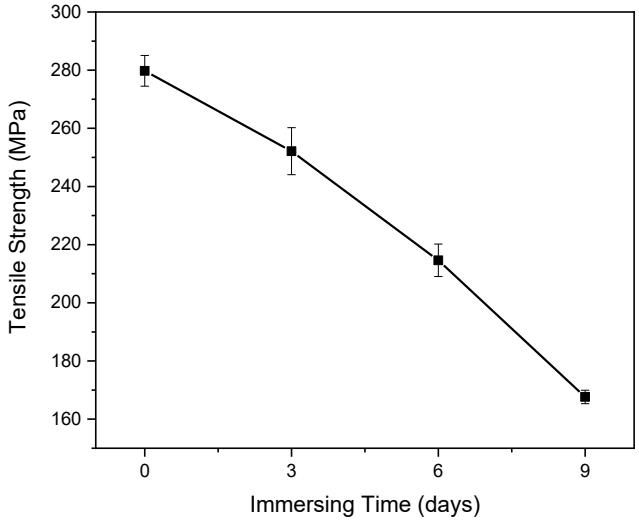

Figure 4. Tensile testing results with immersion time in SBF solution

Table 2. Tensile test results of the samples

Immersion (Days)	Max Force (N)	Yield Strength (MPa)	Tensile Strength (MPa)	Strain (%)
0	3337.2 ± 71.26	182.81 ± 2.84	279.77 ± 5.30	13.74 ± 0.31
3	3025.63 ± 96.83	175.81 ± 5.37	252.14 ± 8.07	13.91 ± 0.96
6	2545.30 ± 11.54	150.39 ± 0.76	214.61 ± 5.58	10.67 ± 1.49
9	2018.30 ± 16.46	134.71 ± 6.02	167.64 ± 2.31	8.66 ± 0.77

In this context, it is important to compare the observed degradation behavior of AZ31B with that of other magnesium alloys. Compared with other magnesium-based alloys, AZ31 magnesium, which has a chemical composition similar to AZ31B, has been reported to exhibit better corrosion resistance than ZK60, which is more susceptible to pitting corrosion, whereas AZ31 tends to undergo filiform corrosion [30]. Nevertheless, the corrosion rate obtained in the present study remains relatively higher than that of the AZ91 magnesium alloy [31]. Several previous studies have also demonstrated that the corrosion resistance of magnesium alloys can be significantly enhanced through the application of surface coating treatments [32]. Therefore, the relatively rapid strength degradation of AZ31B observed in this study can be attributed to its intrinsically lower corrosion resistance, which accelerates the initiation and propagation of

pitting corrosion and effectively reduces the load-bearing cross-sectional area. This comparative analysis underscores the novelty of the present study in providing time-dependent quantitative data on the tensile strength degradation of AZ31B, which remains limited in the existing literature, particularly with respect to implant performance during the critical early stage of bone healing.

Figure 5 illustrates the changes in pH values in the SBF solution during the immersion process. The variation in pH values results from the alteration of hydrogen content caused by the reaction between the metal and the SBF solution. This reaction leads to a significant increase in pH values in the first five days, stabilizing in the subsequent days [33]. The reaction between H_2O and Mg can be considered an oxidation-reduction process, where the anodic reaction involves the transformation of Mg into $Mg^{2+,}$ while the cathodic reaction involves hydrogen evolution. In this context, H_2O accepts electrons to produce H_2 and OH^-, and the formation of OH^- contributes to the pH increase in the immersion solution. Subsequently, Mg^{2+} reacts with OH^- to form $Mg(OH)_2$ [34]. In the final stage, the corrosion product $Mg(OH)_2$ serves as a protective layer, while the pH value of the solution gradually decreases to reach a stable level.

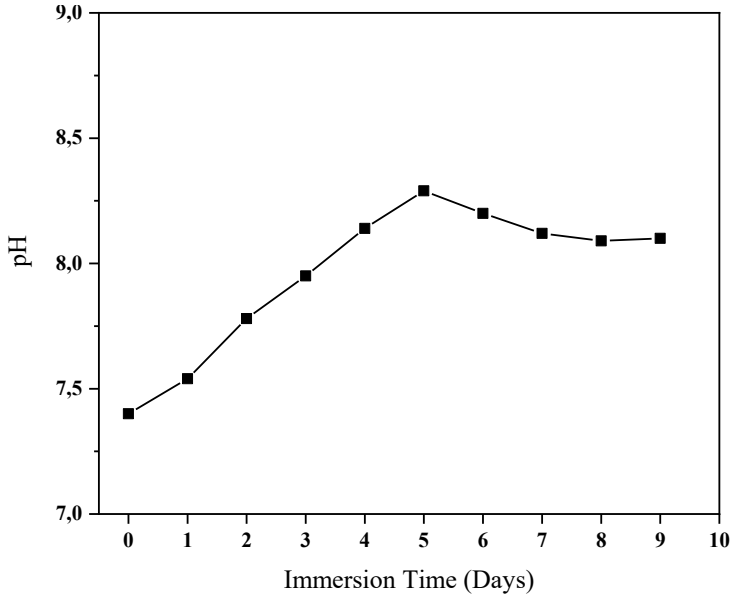

Figure 5. Changes in the pH values of the SBF solution during the immersion process

The change in sample weight during the immersion period is illustrated in Figure 6. The unimmersed sample had an initial weight of 5.164 g and exhibited a significant increase in weight during the first 1–3 days of immersion, reaching 5.281 g on day 3. This weight gain is attributed to the formation of $Mg(OH)_2$ corrosion products adhering to the sample surface, resulting in an increase in sample mass [27]. During days 4–6 of immersion, corrosion progressed further, leading to the degradation of $Mg(OH)_2$ particles on the sample surface and a gradual decrease in sample weight. Subsequently, during days 6–9 of immersion, the extensive formation of pitting corrosion caused a more pronounced reduction in sample weight, reaching 5.157 g on day 9. Based on the total mass loss of 7 mg over 9 days and an exposed surface area of 29.2 cm^2, the average corrosion rate was calculated to be approximately 0.027 $mg/cm^2/day$. This value indicates a relatively low corrosion rate, which can be attributed to the static condition of the SBF solution and the continued presence of protective $Mg(OH)_2$ deposits adhering to the metal surface. The corrosion rate increased with prolonged immersion time, consistent with a transition from relatively uniform surface corrosion to localized pitting

corrosion. The highest corrosion rate was observed in the 6–9 day interval, coinciding with extensive pitting formation and a significant deterioration in mechanical properties [35].

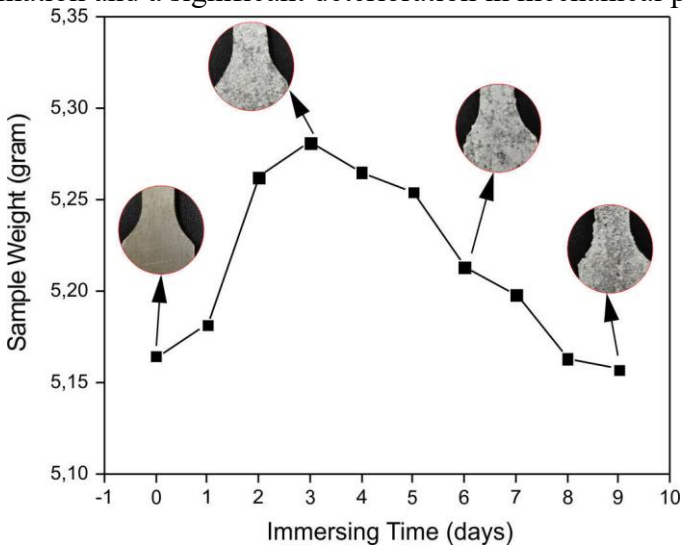

Figure 6. Changes in sample weight over immersion time

Figure 7 shows SEM images of magnesium AZ31B without immersion (Figure 7 (a)) and after immersion in SBF solution for 3-9 days (Figure 7 (b-d)). As seen in Figure 7 (a), the surface morphology without immersion has a uniform structure distribution. In Figure 7 (b), the sample immersed for 3 days begins to experience surface corrosion, starting with the formation of solid clusters adhering to the surface. Additionally, microcracks form, causing the outer layer to fracture and grain boundaries to detach. At this stage, there is an increase in the corrosion rate due to the fracture of the outer layer, forming rectangular blocks with varying sizes. In Figure 7 (c and d), clear evidence of pitting corrosion is observed. The outer layer, already cracked, transforms into micropores. The formation of micropores increases as oxidation protection is lost on the sample surface [34,36]. In Figure 7 (d), fibers resembling unruly hair or blooming flowers are clearly visible. At this stage, the surface structure beneath the pitting corrosion area is distinctly seen, similar to the structure of the sample without immersion. In this case, it can be confirmed that layers are formed during the corrosion process on the surface of magnesium AZ31B metal.

Figure 8 illustrates the corrosion mechanism of AZ31B and its relationship with the reduction in tensile strength during the immersion process. At the initial stage, the magnesium surface is protected by an MgO oxide layer formed through the interaction between the metal and the oxygen-containing environment. As immersion in the SBF solution proceeds, a continuous reaction occurs between dissolved Mg ions and O and H species in the solution, leading to the formation of $Mg(OH)_2$ as the primary corrosion product. This reaction progressively weakens the protective layer and triggers the formation of microcracks in the outer layer. With continued reactions along these microcracks, corrosion evolves into pitting corrosion, resulting in the loss of the oxide layer and the exposure of the underlying surface, while the degraded oxide layer transforms into a microporous structure with broad, flat walls resembling a flower crown [37]. From a mechanical perspective, the formation of corrosion pits and a porous corrosion layer reduces the effective load-bearing cross-sectional area and creates sites of high stress concentration, thereby promoting premature crack initiation under tensile loading and explaining the rapid decline in tensile strength despite relatively small changes in global strain. The clear correlation between the evolution of surface morphology and composition and the mechanical response provides direct mechanistic evidence that corrosion progression plays a dominant role in the loss of structural integrity of the AZ31B magnesium alloy during in vitro testing.

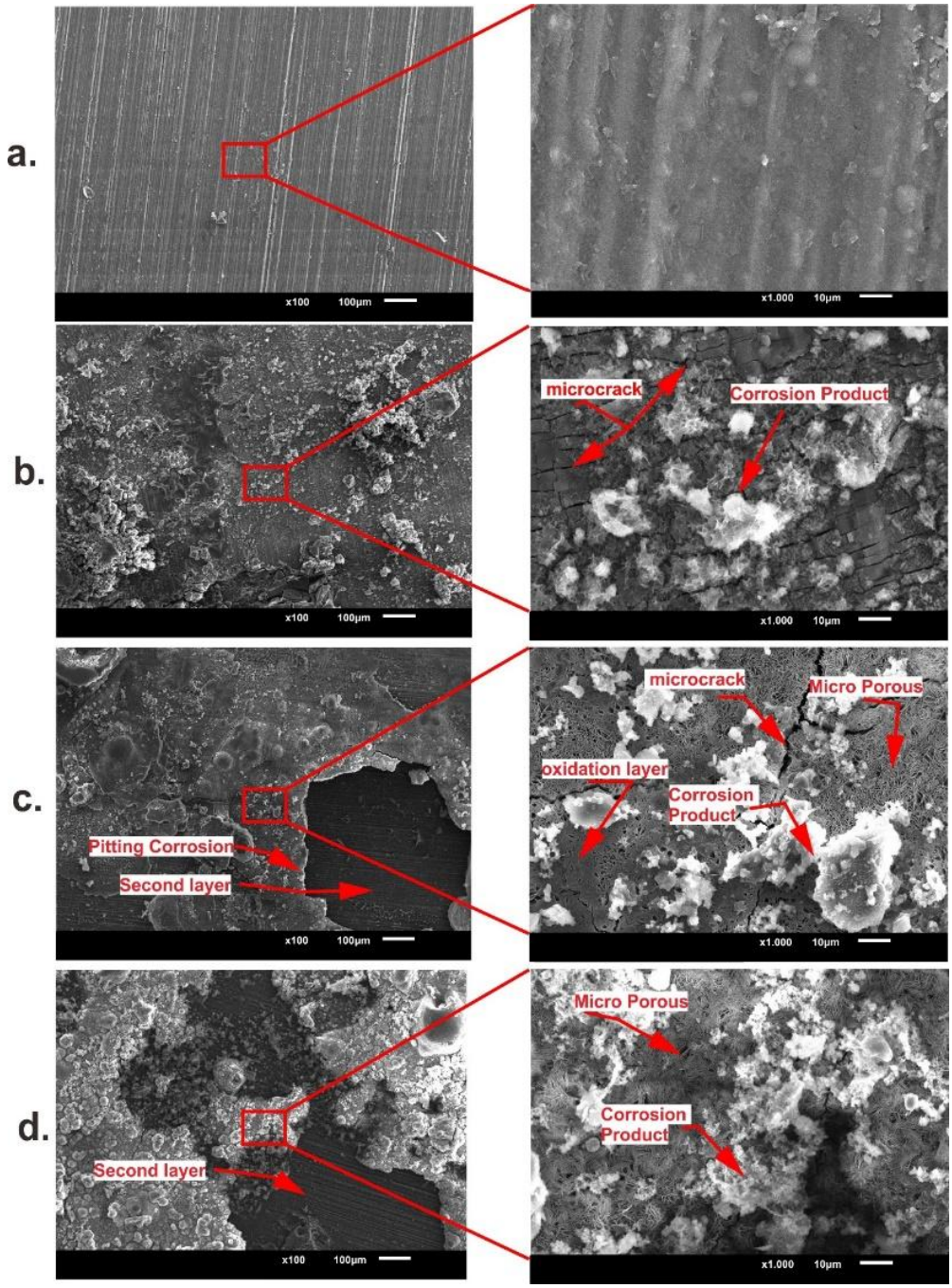

Figure 7. Surface morphology of magnesium AZ31B (a) without immersion, (b) immersed for 3 days, (c) immersed for 6 days, (d) immersed for 9 days

Figure 9 presents the EDX analysis results before (Fig. 9a) and after immersion (Fig. 9b), revealing a transition from an initially relatively homogeneous surface dominated by MgO to a multicomponent corrosion layer after immersion, composed of MgO accompanied by traces of Na_2O, Al_2O_3, SiO_2, P_2O_5, and CaO. This compositional evolution reflects the intensive interaction between the alloy surface and the SBF solution, consistent with medium alkalization and the observed mass loss during immersion. The detection of Ca and P elements within the corrosion layer indicates the possible nucleation of calcium phosphate (CaP)-rich phases, which are commonly associated with enhanced bioactivity and osseointegration potential. However, their non-uniform distribution suggests that the formed CaP layer

is discontinuous and insufficient to provide effective corrosion protection. This allows localized corrosion to persist beneath the partially protective layer, thereby accelerating pitting formation and mechanical degradation. In addition, the reduced intensity of the Al_2O_3 signal at longer immersion times indicates that the surface interface becomes increasingly covered by magnesium corrosion products. From a mechanical perspective, such surface degradation accelerates tensile strength deterioration through a reduction in the effective load-bearing cross-sectional area and the initiation of localized damage. Overall, these findings emphasize the need for interface stabilization through controlled surface engineering strategies, such as pre-treatment or functional coatings, to balance bioactivity and corrosion resistance, as well as the necessity for phase identification and layer thickness verification using X-ray diffraction (XRD) and cross-sectional mapping.

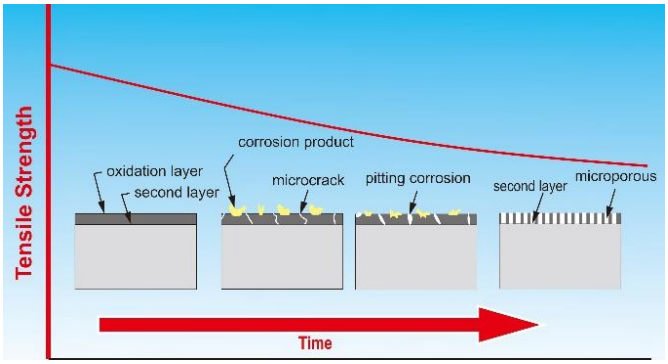

Figure 8. Schematic of the corrosion process of magnesium AZ31B

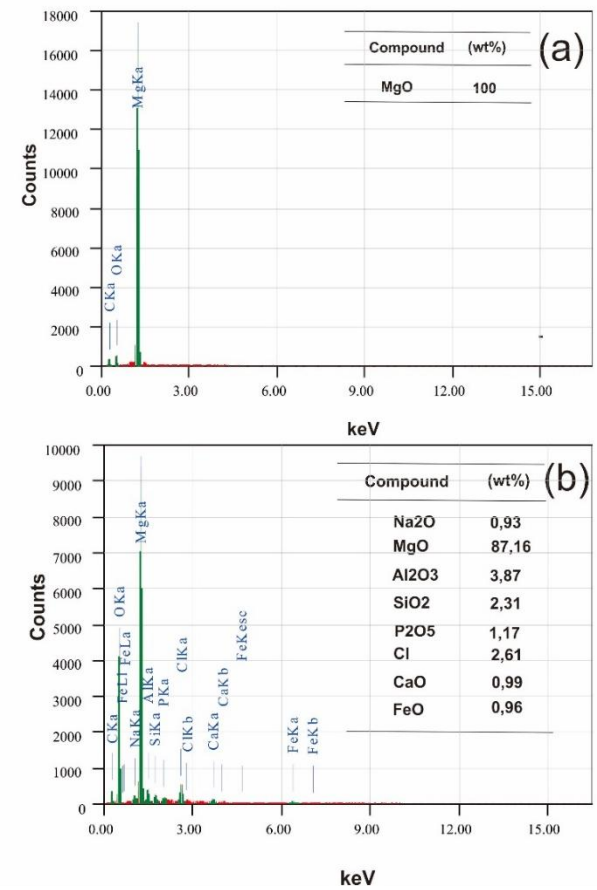

Figure 9. EDX test results (a) without immersion (b) after immersion

4. Conclusions

This study investigates the in vitro degradation behavior of AZ31B magnesium alloy in Simulated Body Fluid (SBF) through tensile testing, surface characterization using SEM–EDX, and pH variation monitoring. Macroscopic observations revealed the formation of white corrosion products on the specimen surfaces, while pitting corrosion became increasingly pronounced after immersion for more than 6 days. The degradation process was initiated by the breakdown of the protective oxide layer, followed by the formation of $Mg(OH)_2$, microcracks, pitting corrosion, and microporous structures, which collectively led to a rapid decline in mechanical performance. Tensile test results demonstrated a progressive reduction in tensile strength of approximately 10%, 23%, and 40% after 3, 6, and 9 days of immersion, corresponding to an average early-stage strength loss of about 4–5% per day. From a mechanical performance perspective, these findings indicate that uncoated AZ31B is not yet suitable for long-term load-bearing biodegradable implant applications, as the rapid loss of tensile strength may compromise structural support before optimal bone healing occurs. Based on the simplified loading assumptions adopted in this study, the effective mechanical safety margin is predicted to decrease significantly during the early implantation period, highlighting the importance of controlling the initial degradation rate. To further complement this research, future studies should prioritize surface modification strategies, such as biodegradable polymer or composite coatings, to delay early-stage degradation and preserve mechanical integrity, supported by phase analysis and corrosion layer thickness evaluation using XRD and cross-sectional SEM mapping, as well as extended-duration in vitro and in vivo investigations under dynamic loading and fluid flow conditions to more realistically represent the physiological environment.

Declaration of AI and AI assisted technologies in the writing process
During the preparation of this work the author(s) used ChatGPT (OpenAI) in order to improve the clarity and readability of the manuscript. After using this tool, the author(s) reviewed and edited the content as needed and take full responsibility for the content of the publication

Declaration of Competing Interest
The authors declare that they have no known competing financial interests or personal relationships that could have appeared to influence the work reported in this paper.

Acknowledgments
The authors would like to express their gratitude to the Department of Mechanical Engineering, Universitas Muhammadiyah Semarang, for the valuable support and facilities provided during the course of this research.

References
[1] Ali S, Irfan M, Niazi UM, Rani AMA, Rashedi A, Rahman S, et al. Microstructure and Mechanical Properties of Modified 316L Stainless Steel Alloy for Biomedical Applications Using Powder Metallurgy. Materials 2022;15. https://doi.org/10.3390/ma15082822.
[2] Gatto ML, Cerqueni G, Groppo R, Santecchia E, Tognoli E, Defanti S, et al. Improved biomechanical behavior of 316L graded scaffolds for bone tissue regeneration produced by laser powder bed fusion. Journal of the Mechanical Behavior of Biomedical Materials 2023;144:105989. https://doi.org/10.1016/j.jmbbm.2023.105989.
[3] Baltatu MS, Vizureanu P, Sandu AV, Solcan C, Hritcu LD, Spataru MC. Research Progress of Titanium-Based Alloys for Medical Devices. Biomedicines 2023;11:2997. https://doi.org/10.3390/biomedicines11112997.
[4] Benea L, Simionescu-Bogatu N. Reactivity and corrosion behaviors of ti6al4v alloy implant biomaterial under metabolic perturbation conditions in physiological solutions. Materials 2021;14. https://doi.org/10.3390/ma14237404.

[5] Vishnu J, Kesavan P, Shankar B, Dembińska K, Swiontek Brzezinska M, Kaczmarek-Szczepańska B. Engineering Antioxidant Surfaces for Titanium-Based Metallic Biomaterials. Journal of Functional Biomaterials 2023;14. https://doi.org/10.3390/jfb14070344.
[6] Li H, Wang M, Lou D, Xia W, Fang X. Microstructural features of biomedical cobalt–chromium–molybdenum (CoCrMo) alloy from powder bed fusion to aging heat treatment. Journal of Materials Science and Technology 2020;45:146–56. https://doi.org/10.1016/j.jmst.2019.11.031.
[7] Lohberger B, Eck N, Glaenzer D, Lichtenegger H, Ploszczanski L, Leithner A. Cobalt chromium molybdenum surface modifications alter the osteogenic differentiation potential of human mesenchymal stem cells. Materials 2020;13:4292. https://doi.org/10.3390/MA13194292.
[8] Tan J, Ramakrishna S. Applications of magnesium and its alloys: A review. Applied Sciences (Switzerland) 2021;11. https://doi.org/10.3390/app11156861.
[9] Nasr Azadani M, Zahedi A, Bowoto OK, Oladapo BI. A review of current challenges and prospects of magnesium and its alloy for bone implant applications. Progress in Biomaterials 2022;11. https://doi.org/10.1007/s40204-022-00182-x.
[10] Amukarimi S, Mozafari M. Biodegradable magnesium-based biomaterials: An overview of challenges and opportunities. MedComm 2021;2:123–44. https://doi.org/10.1002/mco2.59.
[11] Saefudin S, Cahyandari D, Afif IY, Raharjo S, Purnomo P, Amin M. Increasing the Surface Roughness of Magnesium AZ31B using Sandblasting for the Preparation of Biodegradable Implant Materials. AIP Conference Proceedings, vol. 3250, 2025, p. 070006. https://doi.org/10.1063/5.0240666.
[12] Saha S, Lestari W, Dini C, Sarian MN, Hermawan H, Barão VAR, et al. Corrosion in Mg-alloy biomedical implants- the strategies to reduce the impact of the corrosion inflammatory reaction and microbial activity. Journal of Magnesium and Alloys 2022;10:3306–26. https://doi.org/10.1016/j.jma.2022.10.025.
[13] He M, Chen L, Yin M, Xu S, Liang Z. Review on magnesium and magnesium-based alloys as biomaterials for bone immobilization. Journal of Materials Research and Technology 2023;23:4396–419. https://doi.org/10.1016/j.jmrt.2023.02.037.
[14] Candan S, Emir S, Candan E. In Vitro Degradation Behavior of Ti-Microalloyed AZ31 Magnesium Alloy in Simulated Body Fluid. Journal of Materials Engineering and Performance 2022;31. https://doi.org/10.1007/s11665-021-06142-z.
[15] Merino E, El Tawil M, Sobrados I, Durán A, Castro Y. In-vitro degradation behavior of hybrid epoxy-alkyl sol–gel/anodized composite coating on AZ31B Mg alloy. Journal of Sol-Gel Science and Technology 2025;114:139–47. https://doi.org/10.1007/s10971-022-06012-7.
[16] Amin A, Williams B, McGehee T, Navarro A, Patil V, Elsaadany M, et al. In vitro comparative study of composite coatings for magnesium-based bone implants. Results in Surfaces and Interfaces 2025;18. https://doi.org/10.1016/j.rsurfi.2025.100460.
[17] Predoi D, Iconaru SL, Predoi MV, Motelica-Heino M, Buton N, Megier C. Obtaining and characterizing thin layers of magnesium doped hydroxyapatite by dip coating procedure. Coatings 2020;10. https://doi.org/10.3390/COATINGS10060510.
[18] Zhu Y, Liu W, Ngai T. Polymer coatings on magnesium-based implants for orthopedic applications. Journal of Polymer Science 2022;60:32–51. https://doi.org/10.1002/pol.20210578.
[19] Wang G, Wei Y, Hong J, Lv J. Spray-synthesized organic composite/hydroxyapatite coating on magnesium alloys with enhanced corrosion resistance. Frontiers in Chemistry 2025;13. https://doi.org/10.3389/fchem.2025.1566676.
[20] Knigge S, Mueller M, Fricke L, Schilling T, Glasmacher B. In Vitro Investigation of Corrosion Control of Magnesium with Degradable Polycaprolactone Coatings for Cardiovascular Grafts. Coatings 2023;13. https://doi.org/10.3390/coatings13010094.
[21] Hu MH, Yang KC, Chen CW, Chu PH, Chang YL, Sun YH, et al. Multilayer Electrospun-Aligned Fibroin/Gelatin Implant for Annulus Fibrosus Repair: An In Vitro and In Vivo Evaluation. Biomedicines 2022;10. https://doi.org/10.3390/biomedicines10092107.

[22] ASTM B557-15 Standard Test Methods for Tension Testing Wrought and Cast Aluminum- and Magnesium-Alloy Products. ASTM Book of Standards 2016;2.02:1–16.
[23] Kokubo T, Takadama H. Simulated Body Fluid (SBF) as a Standard Tool to Test the Bioactivity of Implants. Handbook of Biomineralization: Biological Aspects and Structure Formation 2008;3:97–109. https://doi.org/10.1002/9783527619443.ch51.
[24] ASTM G31-21. Standard Guide for Laboratory Immersion Corrosion Testing of Metals. ASTM International n.d.
[25] ASTM G1–03. Standard Practice for Preparing, Cleaning, and Evaluating Corrosion Test Specimens. ASTM International 2017.
[26] Xu L, Liu X, Sun K, Fu R, Wang G. Corrosion Behavior in Magnesium-Based Alloys for Biomedical Applications. Materials 2022;15. https://doi.org/10.3390/ma15072613.
[27] Das P, Kumar TSS, Sahu KK, Gollapudi S. Corrosion, stress corrosion cracking and corrosion fatigue behavior of magnesium alloy bioimplants. Corrosion Reviews 2022;40:289–333. https://doi.org/10.1515/corrrev-2021-0088.
[28] Kalatharan SN, Imran AI, Irawan AP, Siregar JP, Cionita T, Fitriyana DF, et al. Mechanical Performance of Alkali-Treated Rattan Strips with Epoxy Coating for Sustainable Composite Applications. Advance Sustainable Science Engineering and Technology 2025;7:02503018. https://doi.org/10.26877/fm53nd79.
[29] Chaudhari YS, Chaudhari MY, Gholap AD, Alam MI, Khalid M, Webster TJ, et al. Surface engineering of nano magnesium alloys for orthopedic implants: a systematic review of strategies to mitigate corrosion and promote bone regeneration. Frontiers in Bioengineering and Biotechnology 2025;13. https://doi.org/10.3389/fbioe.2025.1617585.
[30] Merson E, Poluyanov V, Merson D, Myagkikh P. Corrosion Properties of Biodegradable AZ31 and ZK60 Magnesium Alloys: In Situ Study 2021:3. https://doi.org/10.3390/cmdwc2021-09959.
[31] Bütev Öcal E, Esen Z, Aydınol K, Dericioğlu AF. Comparison of the short and long-term degradation behaviors of as-cast pure Mg, AZ91 and WE43 alloys. Materials Chemistry and Physics 2020;241. https://doi.org/10.1016/j.matchemphys.2019.122350.
[32] Yavuzyegit B, Karali A, De Mori A, Smith N, Usov S, Shashkov P, et al. Evaluation of Corrosion Performance of AZ31 Mg Alloy in Physiological and Highly Corrosive Solutions. ACS Applied Bio Materials 2024;7:1735–47. https://doi.org/10.1021/acsabm.3c01169.
[33] Yu W, Sun R, Guo Z, Wang Z, He Y, Lu G, et al. Novel fluoridated hydroxyapatite/MAO composite coating on AZ31B magnesium alloy for biomedical application. Applied Surface Science 2019;464:708–15. https://doi.org/10.1016/j.apsusc.2018.09.148.
[34] Cheng S, Wang W, Wang D, Li B, Zhou J, Zhang D, et al. An: In vitro and in vivo comparison of Mg(OH)2-, MgF2- and HA-coated Mg in degradation and osteointegration. Biomaterials Science 2020;8:3320–33. https://doi.org/10.1039/d0bm00467g.
[35] Sana A, Malik I, Mujahid M, Akram MA, Adeel Umer M. Surface degradation study of magnesium tested in simulated body fluid. Bio-Medical Materials and Engineering 2019;30:341–8. https://doi.org/10.3233/BME-191057.
[36] Lan X, Zhang J, Wang Z, Zhang R, Sand W, Zhang L, et al. Corrosion of an AZ31B Magnesium Alloy by Sulfate-Reducing Prokaryotes in a Mudflat Environment. Microorganisms 2022;10. https://doi.org/10.3390/microorganisms10050839.
[37] Shen X, Wang Y, Liu Y, Ding J, Zhai Y, Wang M. Preparation of spherical flower-like Mg(OH)2 from waste magnesite and its immobilization performance for Cu2+, Zn2+and Pb2+. Water Science and Technology 2020;82:2536–44. https://doi.org/10.2166/wst.2020.532.